The seal of the University of Delaware, featuring a shield with an open book. The book's pages contain the words 'GRAMM', 'PHILO', 'RHETOR', 'ETHICA' on the left and 'METAPH', 'LOGICA', 'MATHEM', 'PHYSICA' on the right. Below the book is a banner with the word 'SOL'. The seal is surrounded by the Latin motto 'SCIENTIA + 1743 + SINCERITAS' and the words 'UNIVERSITY OF DELAWARE' at the top.

ELEG 404/604 - Digital Image and Audio
Signal Processing

Computed Tomography

Gonzalo R. Arce

Charles Black Evans Professor

Department of Electrical and Computer Engineering
University of Delaware

Spring 2014

X-Ray discovery*

In 1895 Wilhelm Rontgen discovered the X-rays, while working with a cathode ray tube in his laboratory. One of his first experiments was a film of his wife's hand.



*Based on slides from Mark Mirotznik (ELEG 679)



Shoe Fitting X-Ray Device

Shoe stores in the 1920s until the 1970s installed X-ray fluoroscope machines as a promotion device.

CERTIFICATE

SHOE-FITTING TEST DATA FOR _____

1. ANKLE ROLL GOOD FAIR POOR

2. WEIGHT DISTRIBUTION

RIGHT WAY

LEFT RIGHT

—% BALL —%
—% OUTER —%
—% HEEL —%

RIGHT WAY WRONG WAY

3. X-RAY FITTING TEST

RIGHT WAY

LEFT RIGHT

—% BALL —%
—% OUTER —%
—% HEEL —%

RIGHT WAY WRONG WAY

SCIENTIFIC SHOE FITTING AT ITS BEST

On Dr. Scholl's Fluoroscopic Shoe X-ray you can see the position of the bones in your feet right through the shoe. In addition to this checkup other methods of scientific shoe fitting will be employed here during this special demonstration.

GOOD **FAIR** **POOR**

Dr. Scholl's **SHOE FITTING EXPERTS FROM THE CHICAGO FACTORY**

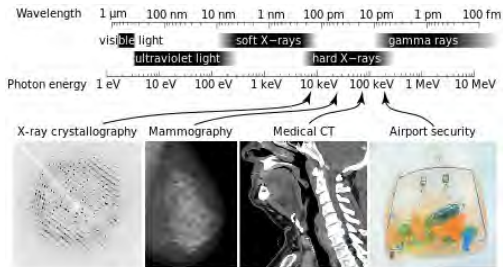
will be in our store
Monday, February 15th

They bring with them the complete line of Dr. Scholl's Shoes (623 fittings) . . . every size, width and style—for every type foot. X-ray fitting—as well as other Dr. Scholl shoe fitting devices. Now you can obtain the shoe that will give you perfect satisfaction—and if you have foot troubles you will be shown how to obtain relief, quickly and inexpensively. Be sure to attend this great **DISPLAY and DEMONSTRATION** . . . first of its kind in this city.

GEO. S. MERCHANT
Winter Garden, Fla.

Oak Ridge Associated Universities
Shoe-Fitting Fluoroscope (ca. 1930-1940)

X-Ray Spectrum

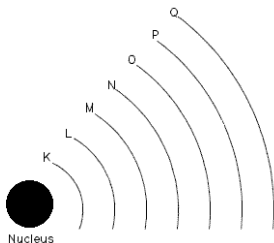


$$E = h \cdot f = h \frac{c}{\lambda}$$

1 eV is the kinetic energy gained by an electron that is accelerated across a one volt potential.

- **Wavelength:** 0.01 - 10 nm.
- **Frequency:** 30 petahertz (3×10^{16}) to 30 exahertz (3×10^{19}).
- **Soft X-Rays:** 0.12 to 30 keV.
- **Hard X-Rays:** 30 to 120 keV.

Electron Binding Energy

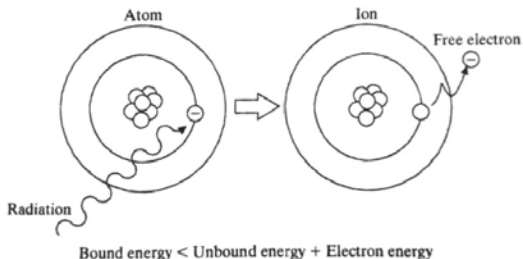


- Electrons are placed into different shells.
- When the ejection of one electron takes place, the energy of the resulting ion added with the energy of the free electron, is greater than the original energy of the atom. That is:

$$\textit{Bound energy} < \textit{Unbound energy} + \textit{Electron energy}$$

- The binding energy is the difference.
- It depends on the element to which the electron is bound.
- Average binding energy of lead 1 keV, tungsten 4 keV, hydrogen 13.6 eV.

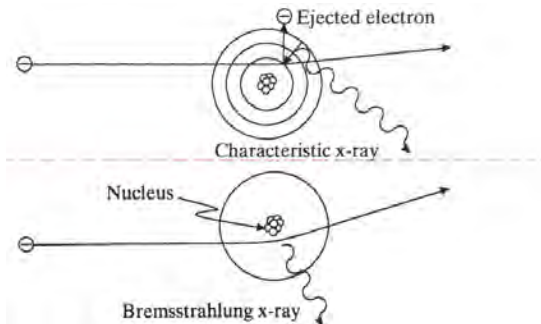
Ionization and Excitation



- **Ionization:** Ejection of an electron from an atom, creating a free electron and an ion. The electron is ejected from the atom if the energy transferred by radiation to it, is equal or greater than the electron's binding energy.
- **Excitation:** Raising of an electron to a higher energy state e.g., an outer orbit.

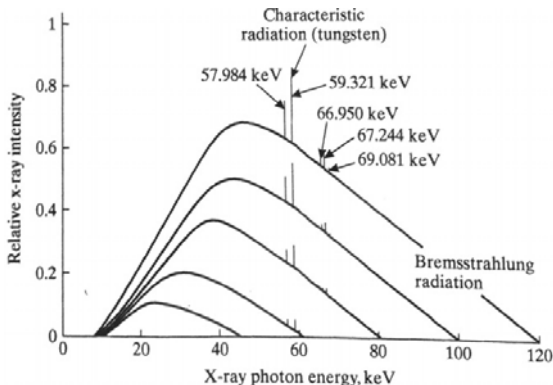


Ionizing Radiation



- **Characteristic X-Ray:** The incident electron collides with a K-shell electron, ionizing the atom. The reorganization generates an x-ray photon which energy depends on the element.
- **Bremsstrahlung Ray:** As the electron approaches the atom, the positive charge of the nucleus causes the incident electron to bend around the nucleus and decelerate. The loss of energy leads to the generation of x-rays. Its the primary source of x-rays from an x-ray tube.

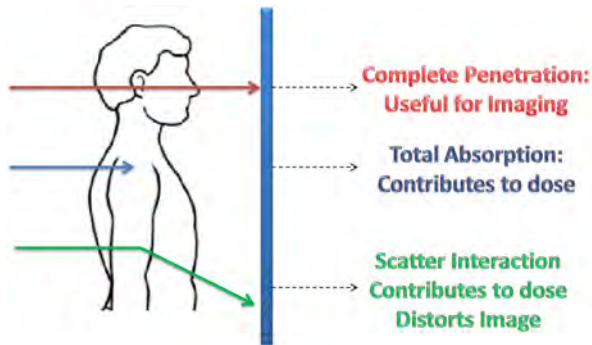
Spectrum of X-Ray



The different curves correspond to different potentials applied to the tube: 45kV, 61kV, 80kV, 100kV and 120 kV. The particular spectral lines correspond to characteristic radiation of Tungsten.



X-Ray interaction with matter

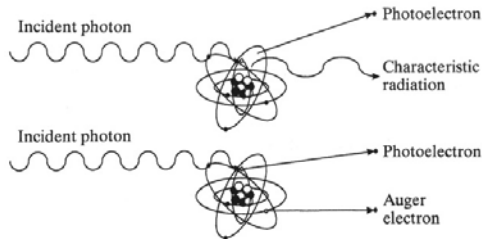


The main mechanisms by which Electromagnetic ionizing radiation interacts with matter are:

- Photoelectric effect
- Compton Scattering
- Coherent Scattering
- Pair Production



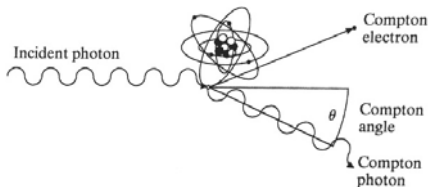
Photoelectric effect



- The photon is not scattered, it is totally absorbed.
- This photon ejects an inner shell electron.
- The ejected electron is called a photoelectron.
- The photoelectric effect is more likely to occur in absorbers of high atomic number (e.g. bone or positive contrast media)
- Contributes significantly to patient dose.
- Responsible for the contrast of the image.



Compton Scattering



- Photon collides with outer-shell electron, producing a new energetic electron called Compton electron.
- The incident photon, the Compton photon, changes its direction and losses energy as a result of the interaction.
- Undesirable for diagnostic radiography, and represents a source of radiation for the personnel conducting the diagnosis.
- It is as likely to occur with soft tissue as bone.



Coherent Scattering and Pair Production

Coherent Scattering

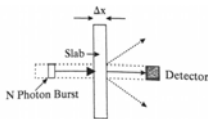
- Also called Thompson, Rayleigh, classical and elastic scattering.
- Incoming X-Ray photon causes an electron to vibrate. This electron emits an X-Ray photon of the same energy but in a different direction.
- Occurs mainly at low X-Ray energies ($< 10\text{keV}$).
- It is generally of little consideration in diagnostic radiography.

Pair Production

- A photon must have at least 1.02 MeV of energy for it to occur.
- The interaction of the photon with the nucleus of the atom produces a pair of particles, an electron and a positively charged positron.
- The energy used for imaging is not of such magnitude, therefore it is not considered for diagnostic radiography.



X-Ray Attenuation



- Photon fluence

$$\Phi = \frac{N}{A}$$

- Photon fluence rate

$$\phi = \frac{N}{A\Delta t}$$

- Energy fluence

$$\Psi = \frac{N\hbar\nu}{A}$$

- Energy fluence rate

$$\psi = \frac{N\hbar\nu}{A\Delta t}$$

- Energy fluence rate is also known as intensity

$$I = E\phi$$

- Considering the homogeneous slab of thickness Δx , and μ as the linear attenuation coefficient, the fundamental photon attenuation law is:

$$N = N_0 e^{-\mu\Delta x}$$

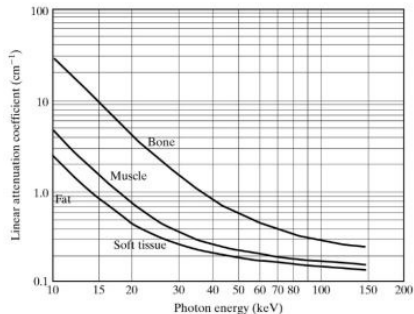
And in terms of intensity:

$$I = I_0 e^{-\mu\Delta x}$$

- N is the number of photons, A denotes area, t denotes time, $\hbar\nu$ is the energy of a photon. N_0 and I_0 are the number of photons at $x=0$ and the intensity of the incident beam respectively.



Linear attenuation coefficient



When the slab is non uniform, that is the linear attenuation coefficient varies along the slab, supposing the mono energetic case:

$$I_d = I_0 e^{-\int_0^d \mu(x(s), y(s)) ds}$$

Where I_d is the xray intensity received of a beam that is projected through a sample along a line s.



Exposure

- Given by the symbol X
- Number of ion pairs produced in a specific volume of air by electromagnetic radiation.
- SI units: C/kg
- Common units: Roentgen, R
- $1\text{C/kg} = 3876\text{ R}$



Dose

- Given by the symbol D
- The general definition is:

$$D = \frac{\text{absorbed energy}}{\text{tissue mass}}$$

- SI units: Grays (Gy) J/kg
- Common units for dose: rad.
- 1 roentgen of exposure yields one rad of absorbed dose in soft tissue.



Dose Equivalent

- Different types of radiation, when delivering the same dose have different effects on the body.
- The symbol H is used

$$H = D \cdot Q$$

- Where Q is the quality factor, determined as a property of the radiation used.e.g. $Q \approx 1$ for x-rays, gamma rays, electrons; $Q \approx 10$ for neutrons and protons; $Q \approx 20$ for alpha particles.
- When D is measured in rads, H is considered to have units rems.
- When D is measured in grays, H is considered to have units sievert (Sv).



Radiation Exposure

The following chart (from the FDA (Food and Drug Administration)) shows radiation exposure from different procedures compared to the background radiation.

Diagnostic Procedure	Typical Effective Dose (mSv) ¹	Number of Chest X rays (PA film) for Equivalent Effective Dose ²	Time Period for Equivalent Effective Dose from Natural Background Radiation ³
Chest x ray (PA film)	0.02	1	2.4 days
Skull x ray	0.1	5	12 days
Lumbar spine	1.5	75	182 days
I.V. urogram	3	150	1.0 year
Upper G.I. exam	6	300	2.0 years
Barlum enema	8	400	2.7 years
CT head	2	100	243 days
CT abdomen	8	400	2.7 years



Biological Effects

- The main risk from ionizing radiation at the doses involved in medical imaging is cancer production.
- Injury to living tissue from the transfer of energy to atoms and molecules of the body.
- Can cause acute effects such as: skin reddening, hair loss and radiation burns.
- The general public should not be exposed to more than 100mrem/year.



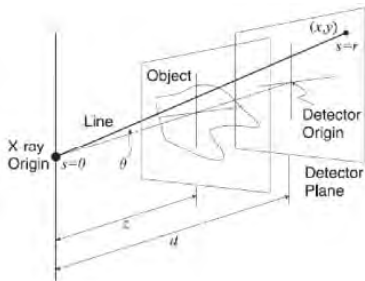
Imaging Equations

Monochromatic X-ray Source:

$$I(x, y) = I_0 e^{-\int_0^{r(x,y)} \mu(s; x, y) ds}$$

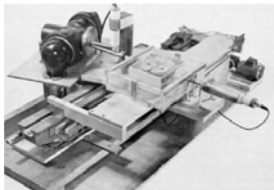
Polychromatic X-ray Source:

$$I(x, y) = \int_{E_{min}}^{E_{max}} S_0(E') E' e^{-\int_0^{r(x,y)} \mu(s; x, y) ds} dE'$$



Reconstruction History

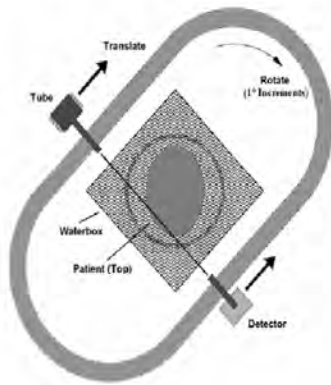
Hounsfield's experimental CT:



- Reconstruction methods based on Radon's work
 - 1917-classic image reconstruction from projections paper
- 1972 - Hounsfield develops the first commercial x-ray CT scanner
- Hounsfield and Cormack receive the 1979 Nobel Prize for their CT contributions
- Classical reconstruction is based on the Radon transform
 - Method known as backprojection
- Alternative approaches
 - Fourier Transform and iterative series-expansion methods
 - Statistical estimation methods
 - Wavelet and other multiresolution methods
 - Sub-Nyquist sampling: Compressed sensing and Partial Fourier Theories

1st Generation CT: Parallel Projections

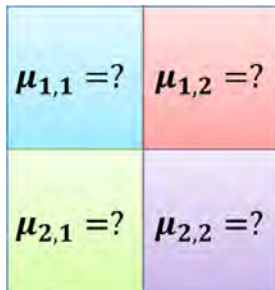
Hounsfield's Experimental CT



- 1 Beam and 1 Detector
- 160 samples/traverse: 5min
- 1° increments over 180°
- 28,800 samples
- Solved simultaneous equations (Fortran): **2.5h**
- 160² image matrix but reduced to 80² for practical clinical use



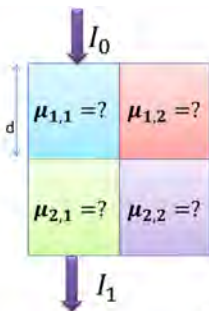
Example



Suppose an object that has 4 materials arranged in the boxes shown above. How can we find the linear attenuation coefficients?



Image Reconstruction



$$I_1 = I_0 e^{-(\mu_{1,1} + \mu_{2,1})d}$$

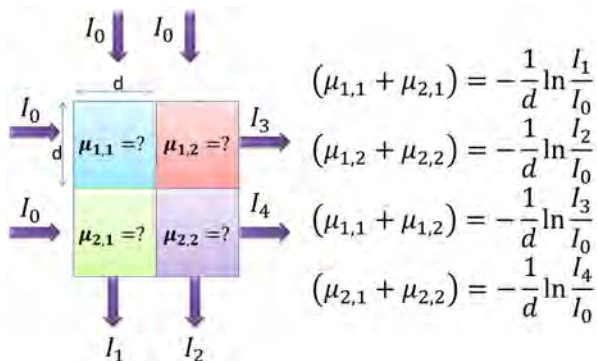
$$\ln \frac{I_1}{I_0} = -(\mu_{1,1} + \mu_{1,2})d$$

$$(\mu_{1,1} + \mu_{1,2}) = -\frac{1}{d} \ln \frac{I_1}{I_0}$$

Suppose an x-ray of intensity I_0 is passing through the first column of the object, and that I_1 is the intensity measured at the other side.



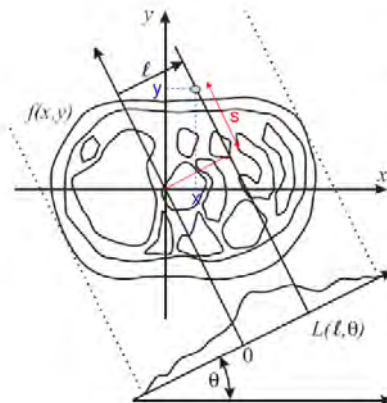
Image Reconstruction



If we repeat the same process for each of the rows and the columns, we obtain the equations necessary to obtain the values of the coefficients. However for bigger systems, the number of equations is not practical for implementation.



Radon Transform



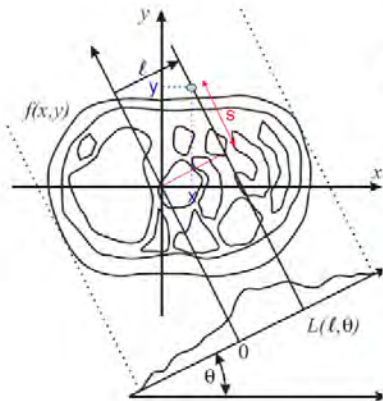
$f(x,y)$ describes our object

We would like to now describe $f(x,y)$ in terms of its projections onto a line $L(l, \theta)$.

Here l is a distance along the line $L(l, \theta)$ starting from the origin.



Radon Transform



$f(x,y)$ describes our object

We would like to now describe $f(x,y)$ in terms of its projections onto a line $L(l, \theta)$.

Here l is a distance along the line $L(l, \theta)$ starting from the origin.

Example: If $\theta=0$

$$g(l, \theta = 0) = \int_{-\infty}^{\infty} f(l, y) dy$$

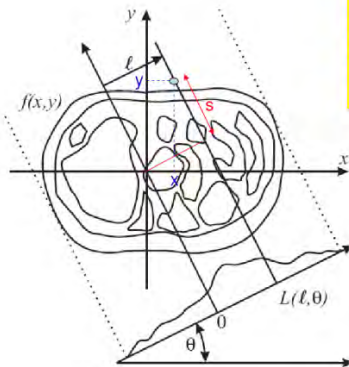
Example: If $\theta=90^\circ$

$$g(l, \theta = 90^\circ) = \int_{-\infty}^{\infty} f(x, l) dx$$



Radon Transform

For Angles different to 0 or 90 degrees.



Option 1: We rotate our coordinate system so that l and the projection direction (axis of integration) are horizontal and vertical

$$x(s) = l \cdot \cos(\theta) - s \cdot \sin(\theta)$$

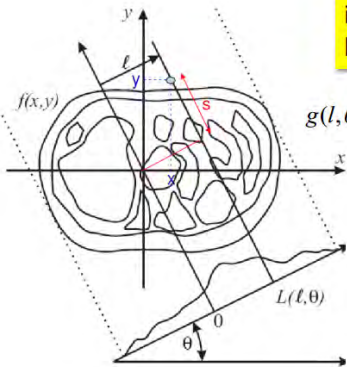
$$y(s) = l \cdot \sin(\theta) + s \cdot \cos(\theta)$$

$$g(l, \theta) = \int_{-\infty}^{\infty} f(x(s), y(s)) ds$$



Radon Transform

Option 2: Instead of rotating the object and integrating we can integrate the object only along the line (L)

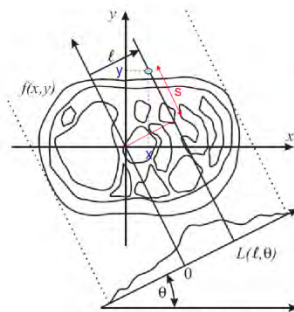


$$g(l, \theta) = \int_{-\infty}^{\infty} \int_{-\infty}^{\infty} f(x, y) \cdot \delta(x \cos \theta + y \sin \theta - l) dx dy$$

$g(l, \theta)$ is called the Radon transform



Radon Transform



$$x(s) = l \cdot \cos(\theta) - s \cdot \sin(\theta)$$

$$y(s) = l \cdot \sin(\theta) + s \cdot \cos(\theta)$$

$$g(l, \theta) = \int_{-\infty}^{\infty} f(x(s), y(s)) ds$$

How does this apply to xrays?

Recall that $I_d = I_o e^{-\int_0^d \mu(x(s), y(s)) ds}$

Is the received xray intensity of a beam that is projected through a sample along the line s

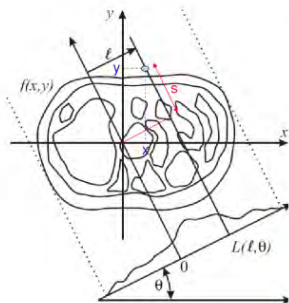
$$-\ln\left(\frac{I_d}{I_o}\right) = \int_0^d \mu(x(s), y(s)) ds$$

Let: $g(l, \theta) = -\ln\left(\frac{I_d}{I_o}\right)$ and $f(x, y) = \mu(x, y)$

we get the radon transform



Radon Transform



Given $g(l, \theta) = -\ln\left(\frac{I_d}{I_o}\right)$ and $f(x, y) = \mu(x, y)$

$$x(s) = l \cdot \cos(\theta) - s \cdot \sin(\theta)$$

$$y(s) = l \cdot \sin(\theta) + s \cdot \cos(\theta)$$

$$g(l, \theta) = \int_{-\infty}^{\infty} f(x(s), y(s)) ds$$

In CT we measure $g(l, \theta) = -\ln\left(\frac{I_d}{I_o}\right)$
and need to find $f(x, y) = \mu(x, y)$

using $g(l, \theta) = \int_{-\infty}^{\infty} f(x(s), y(s)) ds$

$$x(s) = l \cdot \cos(\theta) - s \cdot \sin(\theta)$$

$$y(s) = l \cdot \sin(\theta) + s \cdot \cos(\theta)$$

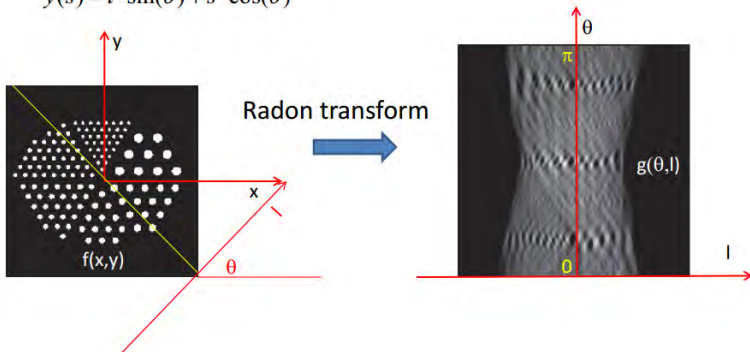
Sinogram

A sinogram is an image of $g(l, \theta)$

$$g(l, \theta) = \int_{-\infty}^{\infty} f(x(s), y(s)) ds$$

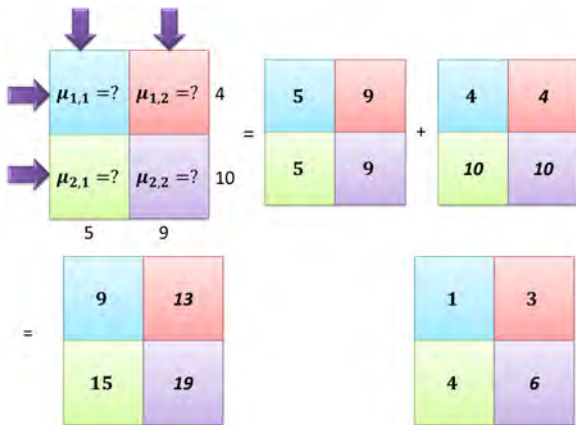
$$x(s) = l \cdot \cos(\theta) - s \cdot \sin(\theta)$$

$$y(s) = l \cdot \sin(\theta) + s \cdot \cos(\theta)$$



Back Projection Example

With the example of the 4 boxes given before, we back project the results obtained. As it can be seen, the right answer is not obtained, however the order of the numbers is the same:



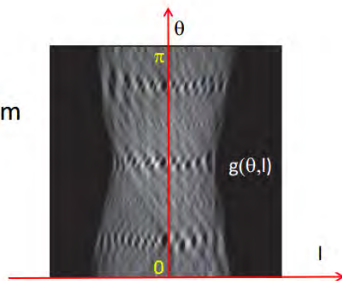
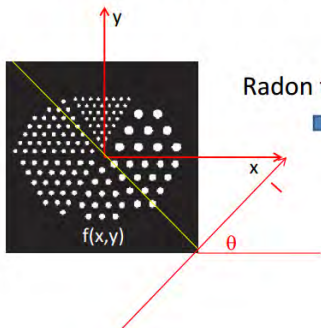
Back Projection Method

A sinogram is an image of $g(l, \theta)$

$$g(l, \theta) = \int_{-\infty}^{\infty} f(x(s), y(s)) ds$$

$$x(s) = l \cdot \cos(\theta) - s \cdot \sin(\theta)$$

$$y(s) = l \cdot \sin(\theta) + s \cdot \cos(\theta)$$

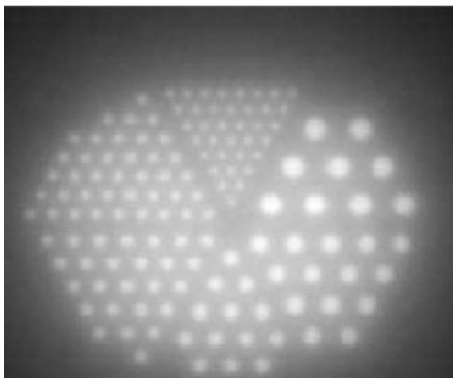


Problems with Back Projection Method

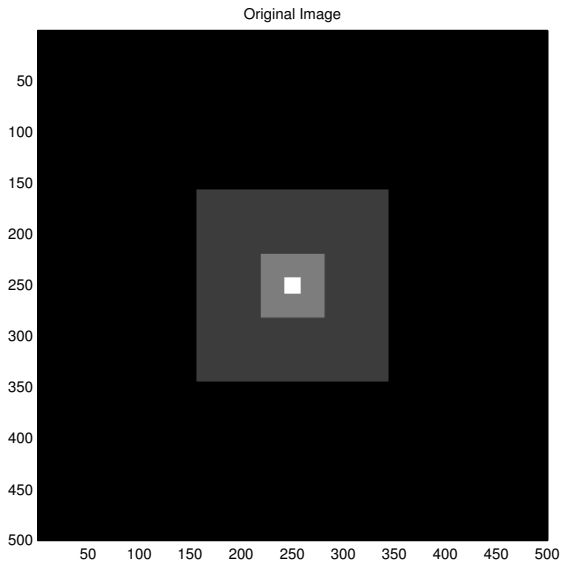
- Bright spots tend to reinforce, which results in a blurry image.
- Problem:

$$f_b(x, y) \neq f(x, y)$$

- Resulting Image:



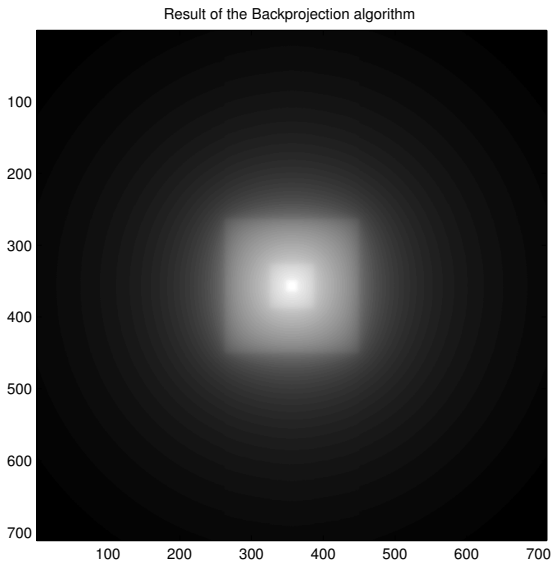
Back Projection Example



Back Projection Example

(Loading Video...)

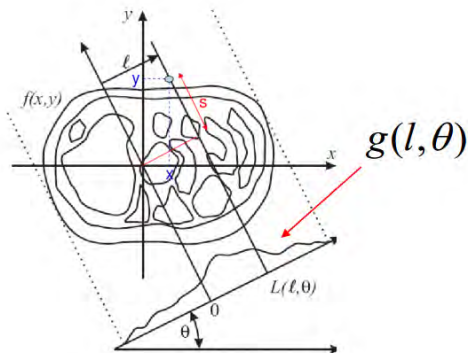
Reconstruction: Back Projection



Projection-Slice Theorem

First take the 1D Fourier transform of a projection $g(l, \theta)$

$$G(\rho, \theta) = \mathfrak{F}_{1D} \{g(l, \theta)\} = \int_{-\infty}^{\infty} g(l, \theta) e^{-j2\pi\rho l} dl$$



Projection-Slice Theorem

From the 1D Fourier transform of a projection $g(l, \theta)$

$$G(\rho, \theta) = \mathfrak{F}_{1D} \{g(l, \theta)\} = \int_{-\infty}^{\infty} g(l, \theta) e^{-j2\pi\rho l} dl$$

Next we substitute the Radon transform for $g(l, \theta)$

$$g(l, \theta) = \int_{-\infty}^{\infty} \int_{-\infty}^{\infty} f(x, y) \cdot \delta(x \cos \theta + y \sin \theta - l) dx dy$$

$$G(\rho, \theta) = \int_{-\infty}^{\infty} \int_{-\infty}^{\infty} \int_{-\infty}^{\infty} f(x, y) \cdot \delta(x \cos \theta + y \sin \theta - l) e^{-j2\pi\rho l} dx dy dl$$

Next we do a little rearranging

$$G(\rho, \theta) = \int_{-\infty}^{\infty} \int_{-\infty}^{\infty} f(x, y) \left\{ \int_{-\infty}^{\infty} \delta(x \cos \theta + y \sin \theta - l) e^{-j2\pi\rho l} dl \right\} dx dy$$



Projection-Slice Theorem

$$G(\rho, \theta) = \int_{-\infty}^{\infty} \int_{-\infty}^{\infty} f(x, y) \left\{ e^{-j2\pi\rho[x\cos\theta + y\sin\theta]} \right\} dx dy$$

$$G(\rho, \theta) = \int_{-\infty}^{\infty} \int_{-\infty}^{\infty} f(x, y) \left\{ e^{-j2\pi[x\rho\cos\theta + y\rho\sin\theta]} \right\} dx dy$$

What does this look like?

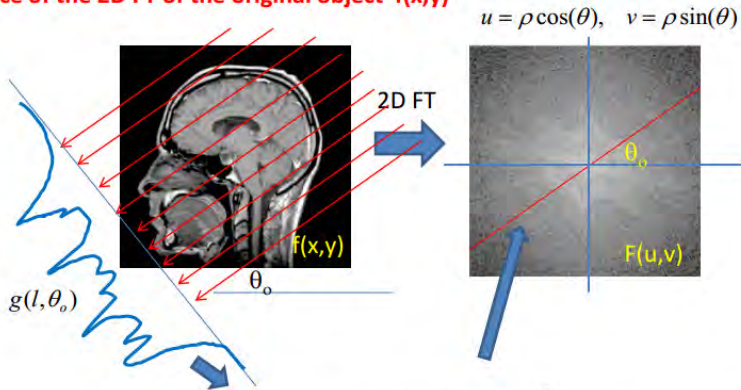
This looks a lot like $F(u, v) = \int_{-\infty}^{\infty} \int_{-\infty}^{\infty} f(x, y) e^{-j2\pi[xu + yv]} dx dy$

with $u = \rho \cos(\theta)$, $v = \rho \sin(\theta)$



Projection-Slice Theorem

If I take the 1D FT of a projection at an angle θ the result is the same as a slice of the 2D FT of the original object $f(x,y)$

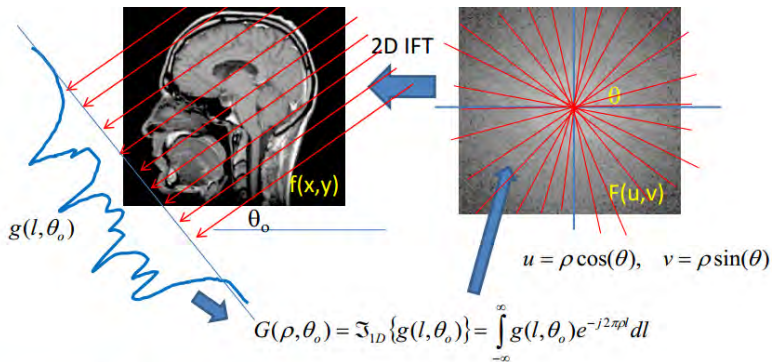


$$G(\rho, \theta_0) = \mathfrak{F}_{1D} \{g(l, \theta_0)\} = \int_{-\infty}^{\infty} g(l, \theta_0) e^{-j2\pi\rho l} dl$$

$$u = \rho \cos(\theta), \quad v = \rho \sin(\theta)$$



Fourier Reconstruction Method



Take projections at all angles θ .

Take 1D FT of each projection to build $F(u,v)$ one slice at a time.

Take the 2D inverse FT to reconstruct the original object based on $F(u,v)$

$$f(x, y) = \mathfrak{F}_{2D}^{-1}\{G(\rho, \theta)\}$$



Fourier Reconstruction Method

- The projection slice theorem leads to the following reconstruction method:
 - Take 1D Fourier Transform of each projection to obtain $G(\rho, \theta)$ for all θ .
 - Convert $G(\rho, \theta)$ to Cartesian grid $F(u, v)$.
 - Take inverse 2D Fourier Transform to obtain $f(x, y)$.
- It is not used because it is difficult to interpolate polar data into a Cartesian grid, and the inverse 2D Fourier Transform is time consuming



Filtered Back Projection

Consider the inverse Fourier Transform in 2D:

In polar coordinates the inverse Fourier transform can be written as

$$f(x, y) = \int_0^{2\pi} \int_{-\infty}^{\infty} F(\rho \cos \theta, \rho \sin \theta) e^{j2\pi\rho[x \cos \theta + y \sin \theta]} \rho d\rho d\theta$$

with $u = \rho \cos(\theta)$, $v = \rho \sin(\theta)$

From the projection theorem $G(\rho, \theta) = F(\rho \cos(\theta), \rho \sin(\theta))$

We can write this as
$$f(x, y) = \int_0^{2\pi} \int_{-\infty}^{\infty} G(\rho, \theta) e^{j2\pi\rho[x \cos \theta + y \sin \theta]} \rho d\rho d\theta$$



Filtered Back Projection

Since $g(l, \theta) = g(-l, \theta + \pi)$ you can show

$$f(x, y) = \int_0^{\pi} \int_{-\infty}^{\infty} G(\rho, \theta) e^{j2\pi\rho[x\cos\theta + y\sin\theta]} |\rho| d\rho d\theta$$

which can be rewritten as

$$f(x, y) = \int_0^{\pi} \left[\int_{-\infty}^{\infty} G(\rho, \theta) e^{j2\pi\rho l} |\rho| d\rho \right]_{l=x\cos(\theta)+y\sin(\theta)} d\theta$$



Filtered Back Projection

- Filter Response.
 - $c(\rho) = |\rho|$.
 - High pass filter.
- $G(\rho, \theta)$ is more densely sampled when ρ is small.
- The ramp filter compensate for the sparser sampling at higher ρ .

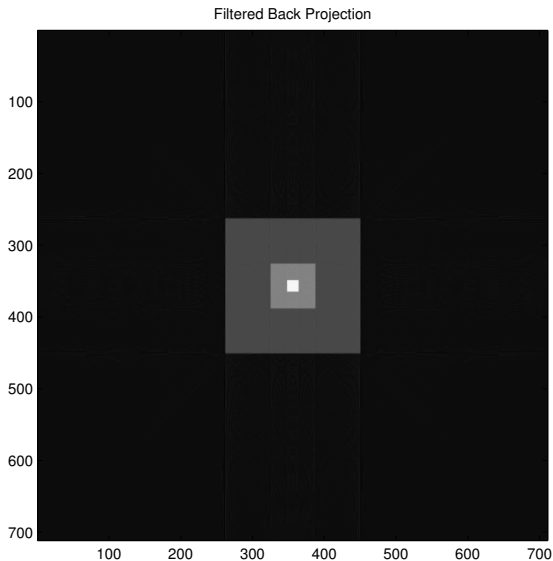


Filtered Back Projection Example

(Loading Video...)



Reconstruction: Filtered Back Projection



Back Projection Method Vs Filtered Back Projection

A. Back Projection

$$b_{\theta}(x, y) = g(x \cos(\theta) + y \sin(\theta), \theta)$$

$$f_b(x, y) = \int_0^{\pi} b_{\theta}(x, y) d\theta$$

B. Filtered Back Projection

$$G(\rho, \theta) = \mathfrak{F}_{1D} \{g(l, \theta)\} = \int_{-\infty}^{\infty} g(l, \theta) e^{-j2\pi\rho l} dl$$

$$f(x, y) = \int_0^{\pi} \left[\int_{-\infty}^{\infty} G(\rho, \theta) e^{j2\pi\rho l} |\rho| d\rho \right]_{l=x \cos(\theta) + y \sin(\theta)} d\theta$$



Convolution Back Projection

From the filtered back projection algorithm we get

$$f(x, y) = \int_0^{\pi} \left[\int_{-\infty}^{\infty} G(\rho, \theta) e^{j2\pi\rho l} |\rho| d\rho \right]_{l=x\cos(\theta)+y\sin(\theta)} d\theta$$

It may be easier computationally to compute the inner 1D IFT using a convolution

recall $\mathfrak{F}_{1D}^{-1}[F_1(\omega) \cdot F_2(\omega)] = f_1(x) * f_2(x)$

$$\Rightarrow f(x, y) = \int_0^{\pi} \left[g(l, \theta) * \mathfrak{F}_{1D}^{-1}(|\rho|) \right]_{l=x\cos(\theta)+y\sin(\theta)} d\theta$$



Convolution Back Projection

$$f(x, y) = \int_0^{\pi} \left[g(l, \theta) * \mathfrak{F}_{1D}^{-1}(|\rho|) \right]_{l=x \cos(\theta)+y \sin(\theta)}$$

Let

$$c(l) = \mathfrak{F}_{1D}^{-1}(|\rho|)$$

$$f(x, y) = \int_0^{\pi} \left[g(l, \theta) * c(l) \right]_{l=x \cos(\theta)+y \sin(\theta)} d\theta$$

The problem is $c(l) = \mathfrak{F}_{1D}^{-1}(|\rho|) = \int_{-\infty}^{\infty} |\rho| e^{j2\pi\rho l} d\rho$ does not exist



Convolution Back Projection

The solution $\tilde{c}(l) = \mathfrak{F}_{1D}^{-1}(|\rho| \cdot W(\rho)) = \int_{-\infty}^{\infty} |\rho| \cdot W(\rho) e^{j2\pi\rho l} d\rho$

where $W(\rho)$ is called a weighting function

$$f(x, y) = \int_0^{\pi} [g(l, \theta) * \tilde{c}(l)] d\theta$$

$$\tilde{c}(l) = \mathfrak{F}_{1D}^{-1}(|\rho| \cdot W(\rho)) = \int_{-\infty}^{\infty} |\rho| \cdot W(\rho) e^{j2\pi\rho l} d\rho$$



Convolution Back Projection

$$f(x, y) = \int_0^{\pi} [g(l, \theta) * \tilde{c}(l)] d\theta$$

$$\tilde{c}(l) = \mathfrak{F}_{1D}^{-1}(|\rho| \cdot W(\rho)) = \int_{-\infty}^{\infty} |\rho| \cdot W(\rho) e^{i2\pi\rho l} d\rho$$

Common windows

- Hamming window
- Lanczos window (Sinc function)
- Simple rectangular window
- Ram-Lak window
- Kaiser window
- Shepp-Logan window

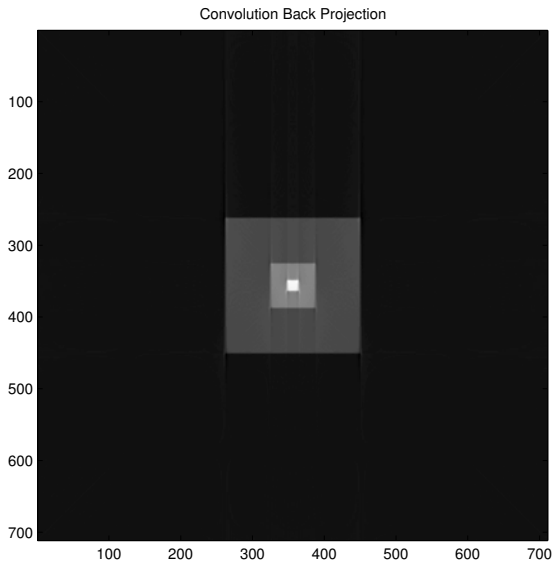


Convolution Back Projection Example

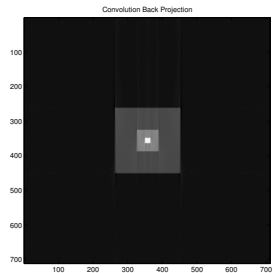
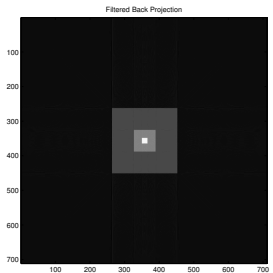
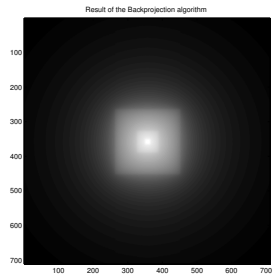
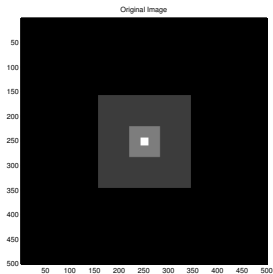
(Loading Video...)



Reconstruction: Convolution Back Projection

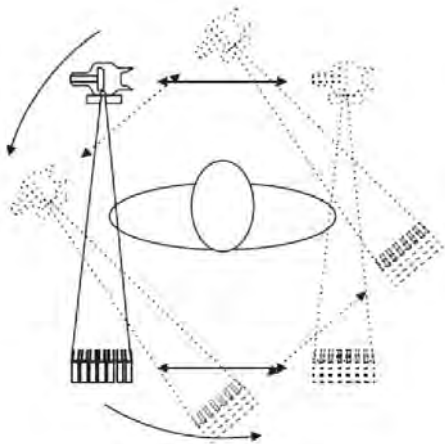


Reconstructions Comparison



2nd Generation

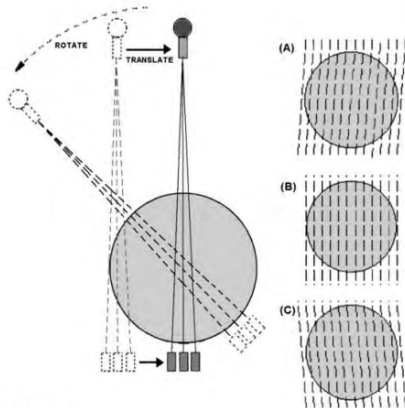
- Incorporated linear array of 30 detectors
- More data acquired to improve image quality
- Shortest scan time was 18 seconds/slice
- Narrow fan beam allows more scattered radiation to be detected



2nd Generation

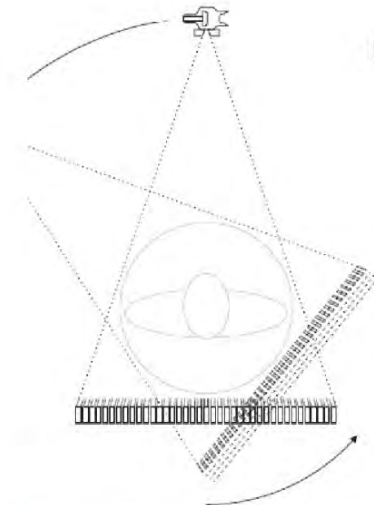


- Multiple detectors
- Still translate-rotate
 - 1 view acquired per detector ($\sim 1^\circ$ apart)
 - angular increment increased by using more detectors



3rd Generation

- Number of detectors increased substantially (more than 800 detectors)
- Angle of fan beam increased to cover entire patient (no need for translational motion)
- Mechanically joined x-ray tube and detector array rotate together
- Newer systems have scan times of 1/2 second



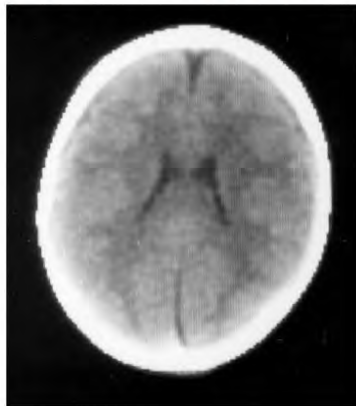
2nd and 3rd Generation Reconstructions

1972: 5 Minutes



2G

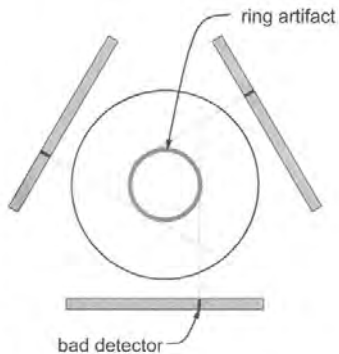
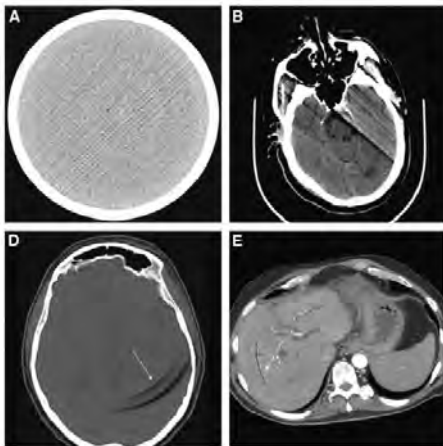
1976: 2 Seconds



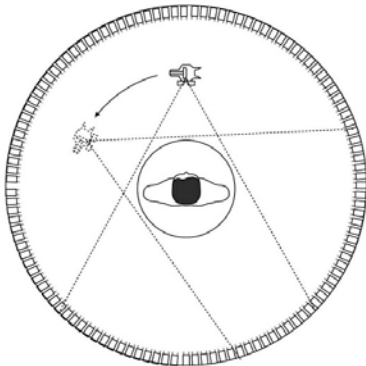
3G

3rd Generation Artifacts

Ring Artifacts



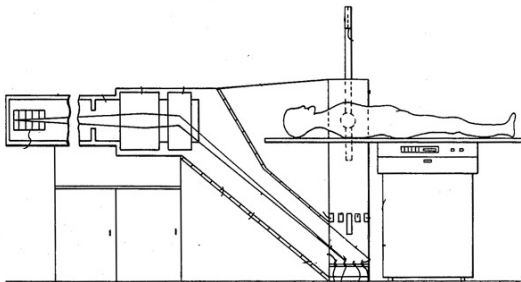
4th Generation



Designed to overcome the problem of artifacts. Stationary ring of about 4800 detectors

5G: Electron Beam CT (EBCT)

- Developed specifically for cardiac tomographic imaging.
- No conventional x-ray tube; large arc of tungsten encircles patient and lies directly opposite to the detector ring
- Electron beam steered around the patient to strike the annular tungsten target.



6G and 7G CT

6G: Electron Beam CT (EBCT)

- Helical CT scanners acquire data while the table moves, there is a single detector array.
- Allows the use of less contrast agent.

7G: Multislice

- CT becomes a cone beam
- 40 parallel detector rows
- 32mm detector length
- 16 0.5mm slices for second

